Schottky barriers to colloidal quantum dot films

Jason P. Clifford, Keith W. Johnston, Larissa Levina, and Edward H. Sargent[a)]
Department of Electrical and Computer Engineering, University of Toronto, Toronto, Ontario M5S 3G4, Canada

(Received 14 August 2007; accepted 20 November 2007; published online 20 December 2007)

We elucidate experimentally a quantitative physical picture of the Schottky barrier formed at the junction between a metallic contact and a semiconducting colloidal quantum dot film. We used a combination of capacitance-voltage and temperature-dependent current-voltage measurements to extract the key parameters of the junction. Three differently processed Al/PbS colloidal quantum dot junction devices provide rectification ratios of 10^4, ideality factors of 1.3, and minimal leakage currents at room temperature. The Schottky barrier height is 0.4 eV and the built-in potential 0.3 V. The depletion width ranges from 90 to 150 nm and the acceptor density ranges from 2×10^{16} to 7×10^{16} cm^{-3}. © *2007 American Institute of Physics*. [DOI: 10.1063/1.2823582]

Solution-processed colloidal quantum dot (CQD) films have recently been shown to offer exceedingly sensitive photodetection,[1] efficient photovoltaic power conversion,[2,3] and controllable switching based on field-effect depletion and accumulation.[4] By virtue of their compatibility with solution processing, CQD films offer the advantage of convenient, low-cost fabrication over large areas and on a wide range of substrates. In addition, quantum-size-effect tuning enables wide-ranging control over bandgap through straightforward modification of synthesis conditions.[5] In principle, the possibility of forming well-controlled Schottky contacts to CQD films, in addition to the ability to form Ohmic contacts, would offer significant benefits in photovoltaic energy conversion and photodetection applications, providing a simple route to efficient electron-hole pair separation via a built-in field.

Previous studies of metallurgical junctions to CQDs include PbS/porous oxide heterojunctions[6,7] and a single-nanocrystal Schottky junction.[8] Here, we focus instead on a detailed investigation of the canonical Schottky barrier: a planar junction between a semiconductor and a metal contact. In our case, the semiconductor consists of a monodispersed colloidal semiconductor film. Although composed of inorganic semiconductor particles and organic insulating molecules, the film is considered to be homogeneous in its macroscopically observable electronic properties. We employ capacitance-voltage (C-V) and temperature-dependent current-voltage measurements (I-V) to determine the key parameters of the Schottky barrier–barrier height, built-in potential, and depletion width–in this materials system. These measurements support a model of device operation wherein hole current flows over a potential barrier in the valence band at the CQD-metal interface, as depicted in the energy band diagram of Fig. 1(b).

We synthesized PbS CQDs capped with 2.5 nm long oleate ligands.[9] The ligands provide colloidal stability and passivate the nanocrystal surfaces. To reduce interparticle spacing in films and improve carrier transport, the original ligands were partially exchanged in favor of shorter primary butylamine ligands.[1] Films (250-nm-thick) were formed by spin-coating CQDs suspended in octane onto commercial glass substrates coated with conductive indium tin oxide (ITO). Aluminum contacts (100-nm-thick and 3.14 mm^2 in area) were deposited on top of this film by thermal evaporation at $\sim1\times10^{-5}$ Torr. A schematic representation of the Al/PbS CQD Schottky barrier device architecture is shown in the inset of Fig. 1(a). All CQD synthesis, processing, and film deposition were carried out in an inert environment with a brief (<30 s) exposure to ambient conditions during trans-

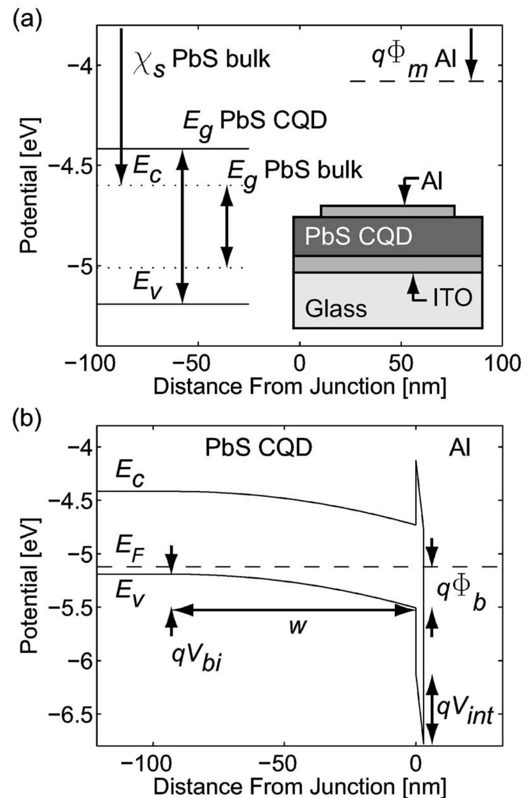

FIG. 1. (a) Valence (E_v) and conduction (E_c) bands of the isolated PbS CQD film (calculated from the electron affinity (χ_s) of bulk PbS and the energy gap (E_g) of the CQD film) and the Fermi energy (E_F) of the Al contact [located by the metal work function ($q\phi_m$)]. The inset shows a schematic view of the Al/PbS CQD Schottky barrier device architecture. (b) Energy bands near the Al/PbS CQD Schottky barrier at zero applied bias (the potential energy scale applies only to the neutral region of the PbS CQD film). See Table I for a description of the Schottky barrier parameters.

[a)]Author to whom correspondence should be addressed. Electronic mail: ted.sargent@utoronto.ca

 © 2007 American Institute of Physics
Author complimentary copy. Redistribution subject to AIP license or copyright, see http://apl.aip.org/apl/copyright.jsp

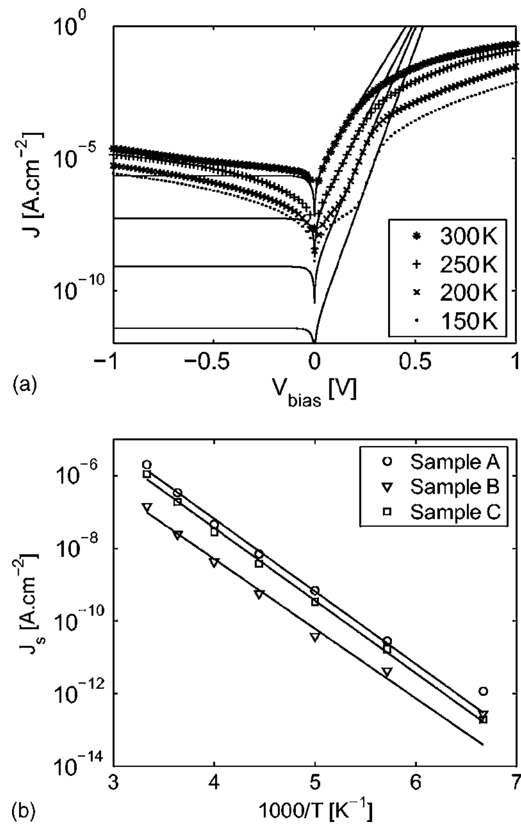

FIG. 2. (a) Measured current-voltage (I-V) characteristics of sample A at 150, 200, 250, and 300 K, and fits of Eq. (1) to the exponential portion of the forward bias currents. (b) Saturation current density vs $1000/T$ for samples A, B, and C.

fer to the vacuum system for metal contact deposition. All measurements were performed in the dark with I-V characterization in an N_2 atmosphere and C-V characterization at room temperature in air.

Figure 2(a) shows the I-V characteristics of an Al/PbS CQD Schottky barrier device at temperatures from 150 to 300 K. Strong rectification was observed at all temperatures. The exponential portion of the forward-bias I-V characteristic (e.g., 0.0–0.3 V at 300 K) is well described by a simple diode equation,

$$J = J_s\left[\exp\left(\frac{qV}{nk_BT}\right) - 1\right], \tag{1}$$

where J_s is the saturation current density, q is the electronic charge, V is the potential drop across the junction, n is the ideality factor, k_B is Boltzmann's constant, and T is the temperature. J_s and n obtained from fitting Eq. (1) to measured I-V characteristics at 300 K for three CQD Schottky barrier devices are provided in Table I.

The saturation current density in Schottky barrier devices is conventionally described within one of two models: thermionic emission theory, which assumes that the carrier populations are at equilibrium throughout the depletion region and that the current-limiting process is the emission of carriers over the energy barrier, and the diffusion theory of emission, which assumes that current is limited by classical carrier transport in the depletion region rather than the emission process.[10] Both theories describe an exponential dependence of J_s on the Schottky barrier height (ϕ_b) and temperature, allowing direct extraction of ϕ_b from temperature-dependent I-V measurements.

We used known or estimated material parameters to predict J_s within each model and found that the diffusion model provided good agreement with the experimentally observed J_s, while the thermionic emission model predicted J_s five orders of magnitude greater than what we observed. This finding is consistent with reports of Schottky barriers formed using other low-mobility semiconductors.[11,12] The reverse-bias characteristics of the CQD Schottky barrier are also better described by the diffusion theory, as the field in the depletion region is dependent on applied bias, resulting in nonsaturating reverse-bias currents.[10]

As shown in Fig. 2(a), at 300 K, in forward bias up to ~0.3 V, the I-V characteristics of the Schottky barrier device are well-described by the simple diode model. At higher biases, a roll-off from the exponential I-V relationship is attributable to series resistance in the bulk of the semiconductor and contacts. The reverse-bias current shows nonsaturating behavior with a magnitude that exceeds the diode saturation current by tenfold at −1.0 V. At low temperatures, the magnitude of the thermionic forward-bias current is reduced, revealing the nonsaturating currents contributing symmetrically to both forward and reverse currents (e.g., −1.0–0.2 V at 150 K) at magnitudes up to a million-fold greater than the saturation current associated with the simple diode model. These currents may be attributable to leakage through the Schottky barrier due to inhomogeneities in barrier height and width.[13–15]

We varied the contact materials on both sides of the CQD film in order to identify the source of the asymmetric I-V characteristics. Only when Al was used as one contact, and either ITO or Au used as the other contact, did we observe strong (>10×) rectification. The use of two Au or ITO contacts led to linear I-V and of two Al contacts to highly nonlinear (thresholded) symmetric behavior. Owing to the high ratio of hole-to-electron mobility in PbS CQD films (as attested by their large photoconductive gain),[16,17] electron injection at the Al contact is assumed to be negligible. We conclude that the Al/PbS CQD junction forms the Schottky barrier for hole transport, and that the other junction provides an Ohmic contact to the valence band.

We extracted ϕ_b from the exponential dependence of J_s on the inverse temperature, as shown in Fig. 2(b). The Schottky barrier heights extracted thereby are shown for three devices in Table I. As expected, the Schottky barrier

TABLE I. Al/PbS CQD Schottky barrier parameters.

Sample	$q\phi_b$ (eV)	J_s (A cm^{-2})	n	Rectification	V_{bi} (V)	N_a (cm^{-3})	w (nm)	E_g (eV)	qV_{int} (eV)	E_v-E_F (eV)
A	0.38	1.7×10^{-6}	1.32	1.1×10^4	0.31	7.1×10^{16}	90	0.73	0.66	−0.07
B	0.38	1.1×10^{-7}	1.28	2.1×10^4	0.28	2.1×10^{16}	150	0.80	0.63	−0.10
C	0.40	1.0×10^{6}	1.35	1.8×10^4	0.33	3.6×10^{16}	120	0.80	0.65	−0.06

Author complimentary copy. Redistribution subject to AIP license or copyright, see http://apl.aip.org/apl/copyright.jsp

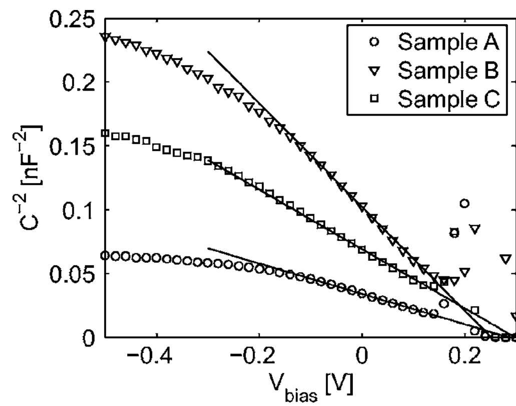

FIG. 3. Measured capacitance as a function of bias (*C-V*) for samples A, B, and C. Measurements were performed with a 10 mV probe signal modulated at 20 Hz.

heights obtained in the present study of quantum-confined materials are larger than those reported for bulk lead chalcogenide Schottky barriers,[18,19] owing to the larger bandgap of the CQDs. The ideality factors for the Al/PbS CQD Schottky devices (~1.3) are closer to unity than in bulk lead chalcogenide Schottky barriers (1.6–1.9).[19] These trends are consistent with the view that the use of short passivating ligands is effective in minimizing recombination, tunneling, and inhomogeneities[15] at the metal-semiconductor interface.

We employed *C-V* analysis to obtain the depletion region width and the exposed acceptor density near the Schottky barrier. The junction capacitance is calculated from the depletion approximation,[10]

$$\frac{1}{C^2} = \frac{2}{A^2 q \varepsilon N_a}\left(V_{\mathrm{bi}} - \frac{k_B T}{q} - V\right), \tag{2}$$

where A is the device area, V is the applied bias, and ε is the static permittivity of the semiconductor. Extraction of the acceptor density (N_a) and the built-in potential (V_{bi}) is achieved by fitting Eq. (2) to the measured capacitance over a range of applied biases. The static permittivity of the PbS CQD film was obtained from the Schottky barrier devices using the carrier extraction by linearly increasing voltage technique (CELIV).[20] Measurements of devices fabricated with a selection of CQD batches yielded a static relative permittivity of 17 ± 2.[3] We show in Fig. 3 the measured capacitance as a function of applied bias for three Al/PbS CQD Schottky barrier devices. Extracted values of V_{bi} and N_a for these devices are provided in Table I. We also tabulate the depletion width at zero bias (w).

We summarize in Fig. 1 our interpretation of the energetic relationship between the semiconducting PbS CQD film and the metal contact. Figure 1(a) shows locations of the energy bands of the isolated CQD film and the work function ($q\phi_m$) of metallic aluminum (4.1 eV). We situate the conduction and valence band edges in the CQD film based on a bulk PbS electron affinity (χ_s) of 4.6 eV,[21,22] and assume equal displacement of both bands due to the quantum confinement in a semiconductor with equal electron and hole effective masses.[23] The CQD film is treated as a homogeneous medium, consistent with the smooth, continuous macroscopic electronic properties observed in the CQD Schottky barrier devices.

Figure 1(b) shows the proposed energy bands in the vicinity of the Al/PbS CQD junction at thermal equilibrium and zero applied bias. The height of the Schottky barrier is predicted within Schottky-Mott theory to be ~1.0 eV based on the calculated difference in work functions of the two materials;[10] however, the barrier heights extracted experimentally herein are ~0.4 eV. We account for the additional potential drop across the junction (V_{int}) by positing a thin interfacial layer at the junction, and localized charge on the surface of the semiconductor per the Bardeen Schottky barrier model.[10] The magnitude of V_{int} depends directly on χ_s and may be smaller for PbS surfaces free of oxidation.[22]

Within the spatial energy band diagram of Fig. 1(b) it is possible to check for self-consistency by calculating the distance between the Fermi energy and the valence band edge ($E_v - E_F$) based on two methods: solving E_F for charge neutrality ($p_0 = N_a$) far from the junction or taking $E_F = E_V - qV_{\mathrm{bi}} + q\phi_b$. For each of the devices in Table I, the location of the calculated Fermi energies agreed within ~0.05 eV.

We have presented detailed measurements of the physical parameters of the Schottky barrier formed at the interface of a semiconducting colloidal quantum dot film and a metal contact. These measurements support a model of device operation based on hole transport restricted by a potential barrier in valence band at the metallurgical junction.

The authors wish to thank Dr. Andras G. Pattantyus-Abraham, Gerasimos Konstantatos, and Dr. Sjoerd Hoogland for many discussions during the course of this study.

[1] G. KCompanyonstantatos, I. Howard, A. Fischer, S. Hoogland, J. Clifford, E. Klem, L. Levina, and E. H. Sargent, Nature (London) **442**, 180 (2006).
[2] I. Gur, N. A. Fromer, M. L. Geier, and A. P. Alivisatos, Science **310**, 462 (2005).
[3] K. W. Johnston, A. G. Pattantyus-Abraham, J. P. Clifford, S. H. Myrskog, D. D. MacNeil, S. Hoogland, H. Shukla, E. J. D. Klem, L. Levina, and E. H. Sargent (unpublished).
[4] D. V. Talapin and C. B. Murray, Science **310**, 86 (2005).
[5] E. H. Sargent, Adv. Mater. (Weinheim, Ger.) **17**, 515 (2005).
[6] K. K. Nanda and S. N. Sahu, Appl. Phys. Lett. **79**, 2743 (2001).
[7] R. Konenkamp, P. Hoyer, and A. Wahi, J. Appl. Phys. **79**, 7029 (1996).
[8] M. C. Newton, S. Firth, and P. A. Warburton, Appl. Phys. Lett. **89**, 072104 (2006).
[9] M. A. Hines and G. D. Scholes, Adv. Mater. (Weinheim, Ger.) **15**, 1844 (1993).
[10] E. H. Rhoderick and R. H. Williams, *Metal-Semiconductor Contacts* (Clarendon, Oxford, 1988).
[11] A. Assadi, C. Svensson, M. Willander, and O. Inganas, J. Appl. Phys. **72**, 2900 (1992).
[12] M. Campos and B. Bello, Jr., J. Phys. D **26**, 1274 (1993).
[13] T. Hashizume, J. Kotani, and H. Hasegawa, Appl. Phys. Lett. **84**, 4884 (2004).
[14] H. Saitoh, T. Kimoto, and H. Matsunami, Mater. Sci. Forum **457**, 997 (2004).
[15] R. T. Tung, Phys. Rev. B **45**, 13509 (1992).
[16] F. Stockmann, Appl. Phys. **7**, 1 (1975).
[17] A. Rose, *Concepts in Photoconductivity and Allied Problems* (Krieger, Huntington, NY, 1978).
[18] J. Baars, D. Bassett, and M. Schulz, Phys. Status Solidi A **49**, 483 (1978).
[19] S. Kumar, Z. H. Khan, M. A. M. Khan, and M. Husain, Curr. Appl. Phys. **5**, 561 (2005).
[20] G. Juska, K. Arlauskas, and M. Viliunas, Phys. Rev. Lett. **84**, 4946 (2000).
[21] R. A. Knapp, Phys. Rev. **132**, 1891 (1963).
[22] R. M. Oman and M. J. Priolo, J. Appl. Phys. **37**, 524 (1966).
[23] K. K. Nanda, F. E. Kruis, and H. Fissan, J. Appl. Phys. **95**, 5035 (2004).

Author complimentary copy. Redistribution subject to AIP license or copyright, see http://apl.aip.org/apl/copyright.jsp